Photoinduced Electron Transfer in Bisporphyrin – Diimide Complexes

Lucia Flamigni,*[a] Martin R. Johnston,*[b, c] and Lingamallu Giribabu[b]

Abstract: The bisporphyrin host **ZnH** was synthesized, and its complexation with two aromatic diimide guest molecules, bis(pyridyl)naphthalenediimide **NIN** and bis(pyridyl)phenyldiimide **PIN**, was investigated by ^{1}H NMR and UV/Vis spectroscopy. The diimide guests were complexed simultaneously with both metalloporphyrins of the host, with association constants on the order of $10^8\,\text{M}^{-1}$. The processes occurring in the complex after excitation of the porphyrinic host were studied by steady-state and time-resolved emission and transient absorption spectroscopy. Complexation alters the photophysical properties of the host **ZnH**; the luminescence bands shift to the red by 30 nm in the complexed forms, while the emission quantum yield and the lifetime decrease. Comparison of a complex between **ZnH** and a model guest unable to undergo photoinduced processes allowed us to establish that, in the diimide complexes, quenching of the porphyrinic luminescence occurs with a rate of $1.1 \times 10^{10}\,\text{s}^{-1}$. The process is identified as an electron transfer from the excited singlet of the porphyrinic host to the imide guest, which yields charge-separated states with a lifetime of 710 ps for **ZnH**$^+$-**NIN**$^-$ and 260 ps for **ZnH**$^+$-**PIN**$^-$.

Keywords: electron transfer · host–guest systems · N ligands · photochemistry · porphyrinoids

Introduction

In the last decades, the construction of artificial porphyrinic arrays for solar energy conversion by using noncovalent bonds[1] has paralleled that based on covalent linkages.[2] However, the former approach, which more closely resembles the natural photosynthetic apparatus, in which the photoactive components are positioned by a protein matrix by means of a combination of interactions, has the inconveniences of low association tendency and poor control over geometry. In this respect, a great improvement has been the introduction of a cooperative strategy in which more than one noncovalent interaction gives control over the positioning of chromophores and dramatically increases the association tendency of the components.[3] An advantage in using noncovalently assembled structures is the simple and fast interchange of components within the system; this does not require the lengthy synthetic schemes that the covalent approach does.

A further advantage of noncovalently linked systems for conversion of light energy to chemical energy is the contribution to the photoinduced separation of charges over long distances, which could be provided by movements in the weakly bound noncovalent array. In rigid, covalently linked systems, long-lived charge-separated states are produced by a sequence of vectorial electron transfers that take the electron to an acceptor distant from the donor. A very demanding design and synthesis of covalently assembled triads, tetrads, or even pentads bearing the donor and acceptor at the extremities of long arrays is often necessary to optimize the performance of these systems.[2] When the structure is held together by noncovalent interactions, a further possibility is open in addition to the multistep electron transfer outlined above. The intrinsic lability of bonds can in principle allow, in the presence of a photochemically induced modification that weakens the interaction, the escape[4] or the rearrangement[5] (e.g., rotation or translation) of a component that could greatly contribute to the spatial separation of charges. Great efforts in the design, synthesis, and photophysical characterization are still needed to achieve such a goal, but this possibility makes noncovalently bound arrays very promising for the construction of structures able to perform efficient charge separation.

The systems presented here are based on the axial coordination of the two pyridyl residues of the aromatic

[a] Dr. L. Flamigni
Istituto ISOF-CNR
Via P. Gobetti 101
40129 Bologna (Italy)
Fax: (+39) 051-639-9844
E-mail: flamigni@frae.bo.cnr.it

[b] Dr. M. R. Johnston, Dr. L. Giribabu
Center for Molecular Architecture
Central Queensland University
Rockhampton, Queensland 4702 (Australia)

[c] Dr. M. R. Johnston
Current address:
School of Chemistry, Physics and Earth Sciences
Flinders University, South Australia 5042 (Australia)
Fax: (+61) 8-8201-2905
E-mail: martin.johnston@flinders.edu.au

  0947-6539/02/0817-3938 $ 20.00+.50/0

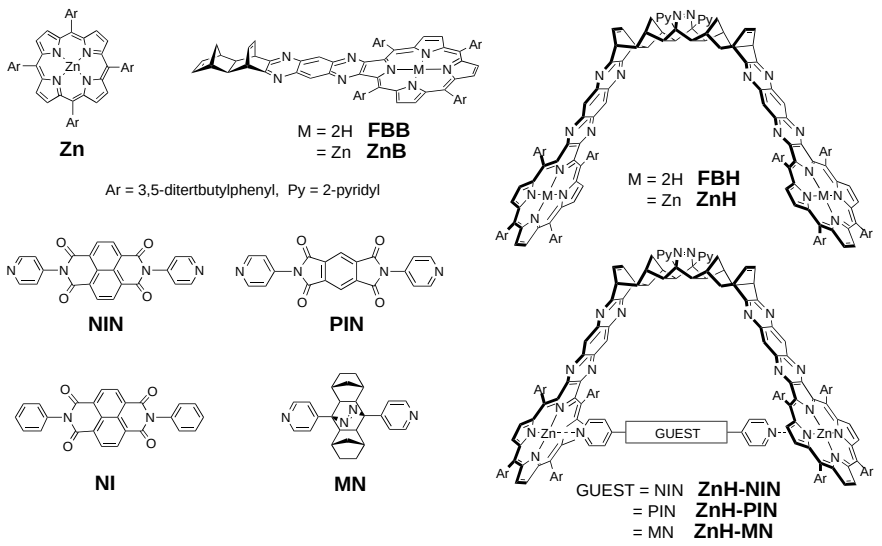

imides **NIN** and **PIN** by the two Zn^{II} ions of the bisporphyrin clamp **ZnH**; due to the close fit of the guests to the cavity and the cooperativity of the two interactions, the systems readily associate.[6] The combination of a good electron donor, such as Zn^{II} porphyrin, and good electron acceptors, such as imides, was expected to provide efficient electron transfer, and we intended to assess the properties of the resulting charge-separated state. While the cations derived from Zn^{II} porphyrins display absorption bands around 650 nm, a region of strong absorbance of singlet and triplet excited states of Zn^{II} porphyrin, the anions derived from aromatic imides by reduction display strong and characteristic absorption features in spectral regions free from interference by other typical components of supramolecular arrays (e.g., porphyrins, fullerenes, carotenoids).[7–11] This feature allows for the unambiguous identification of electron-transfer processes and for the determination of relevant kinetic parameters.

To date only a few reports on photoinduced electron transfer between zinc porphyrins axially connected to imides have thoroughly addressed photoinduced electron transfer across a noncovalent bridge.[12–14] In addition, none of these were characterized by a high association constant *and* a rigidly defined geometry. We previously reported the efficient complexation of the bis(pyridyl)naphthalenediimide **NIN** by **ZnH** and observed quenching of the luminescence of the host, which was tentatively assigned to electron transfer.[6] Here we extend the study to a complex containing bis(pyridyl)phenyldiimide **PIN** and give a detailed account of the spectroscopic (NMR and UV/Vis) and electrochemical characterization of both the components and the complexes involved. In addition, we used time-resolved spectroscopy to fully characterize the electron-transfer processes occurring within the complexes and the resulting charge-separated states.

Results and Discussion

Components

Synthesis: The diimide acceptors **NIN** and **NI** were synthesized from 1,4,5,8-naphthalene bis(anhydride) and 4-aminopyridine or aniline, respectively, in refluxing DMF;[15] **PIN** was synthesized from 1,2,4,5-phenyl bis(anhydride) and 4-aminopyridine in a similar manner.[16] Compound **MN** was isolated from a 4-pyridyl *s*-tetrazine coupling reaction[17] with two molecules of norbornene.[18]

Bis-porphyrin host **ZnH** was synthesized from the norbornenyl-functionalized porphyrin building block **FBB** and 2-pyridyl *s*-tetrazine (Scheme 1).[19] A solution of **FBB** and tetrazine in dichloromethane (DCM) was pressurized at 14 kbar for 20 h and yielded the unmetalated host **FBH** (52% after chromatographic separation). The *s*-tetrazine coupling protocol has been investigated for a variety of norbornenyl-functionalized building blocks and found to proceed stereoselectively.[17] This characteristic, when combined with the defined geometry of the porphyrin block **FBB**, allows the product architecture to be designed with high degree of certainty.

In the ^{1}H NMR spectrum, coupling of block **FBB** to yield host **FBH** results in the loss of the signal for the norbornenyl olefinic proton, as expected for the change in hybridization of the carbon atoms. In addition, the bridge methylene protons H_a and H_b (Scheme 1) are now diagnostic ($\delta = 0.79$ and 1.77 ppm, respectively), since H_a in particular is shifted significantly upfield by the adjacent diaza double bond. In contrast, signals for protons attached to the porphyrin moiety are little affected by the coupling reaction. Mass spectrometry yielded a doubly charged molecular ion at the required position ($m/z = 1465$). Molecular modeling (AM1) of the bisporphyrin cavity clearly showed its overall V shape and gave a porphyrin center-to-center distance of 22 Å.[19]

Metalation of **FBH** with zinc was carried out under standard conditions ($Zn(OAc)_2$, $CHCl_3$/MeOH) to give the bismetalloporphyrin host **ZnH**. The ^{1}H NMR spectrum of **ZnH** is essentially identical to that of **FBH**, with the exception of the signals of the inner porphyrin hydrogen atoms. In addition, the signals for the pyrrole protons adjacent to the

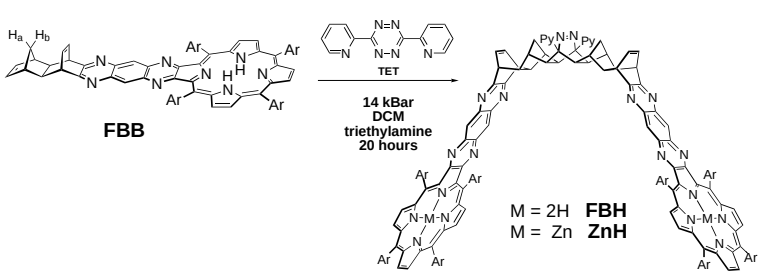

Scheme 1.

  0947-6539/02/0817-3939 $ 20.00+.50/0

quinoxaline substituent are now coincident and are observed as a singlet ($\delta = 8.93$). High-resolution electrospray mass spectroscopy on **ZnH** yielded a doubly charged molecular ion at the required position ($m/z = 1528.317$ [M^{2+}+2 H]) and thus verified the identity of **ZnH**.

Spectroscopy and photophysics: The absorption spectra of host **ZnH** and guest **NIN** in toluene are shown in Figure 1. As reported previously, the absorption spectrum of **ZnH** is twice that of the monoporphyrin component **ZnB**, and this indicates

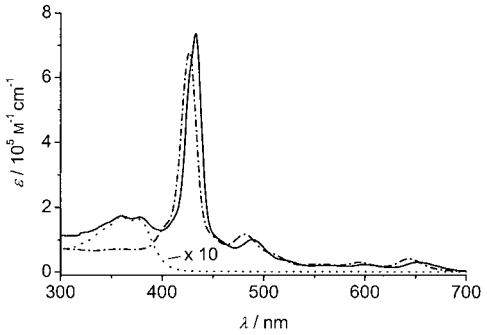

Figure 1. Ground-state absorption spectra of **ZnH** (•–•–), **NIN** (••••), and complex **ZnH-NIN** (——) in toluene. The molar absorption coefficient of **NIN** is multiplied by 10. The spectrum of the complex **ZnH-NIN** was measured with an excess of **NIN**.

that the two porphyrinic extremities of **ZnH** are electronically well separated by the alicyclic backbone.[20] The luminescence spectrum of **ZnH** in toluene displays a maximum at 660 nm with an emission quantum yield of 0.043 and a lifetime of 1.2 ns. The photophysical properties of **ZnH** are profoundly affected by solvent; for example, the emission maximum, quantum yield, and lifetime in DCM are 710 nm, 0.004, and 0.520 ns, respectively.[20] We attributed this solvent dependence to an increase in the dipole moment of the lowest excited singlet state, which is stabilized by polar solvents, in full agreement with the results of semi-empirical calculations. In a glassy toluene solution at 77 K the fluorescence spectrum of **ZnH** has a maximum at 666 nm (lifetime 1.5 ns), and the delayed spectrum has a band at 835 nm (lifetime 12.5 ms), which has been assigned to phosphorescence from the lowest triplet state.[20] On the basis of these results energy levels of 1.86 eV and 1.48 eV can be derived for the lowest singlet and triplet states of **ZnH**, respectively.[21]

The absorbance spectrum of **NIN** (Figure 1) displays bands at 360 nm ($\varepsilon = 1.6 \times 10^4\,\text{M}^{-1}\text{cm}^{-1}$) and at 377 nm ($\varepsilon = 1.7 \times 10^4\,\text{M}^{-1}\text{cm}^{-1}$), in agreement with similar compounds.[22, 23] The emission spectrum of **NIN** in the glass has a band around 410 nm, which allows the singlet energy level to be determined to be approximately 3 eV, well above the energy of the excited state of the porphyrinic component (1.86 eV). By comparison with previously studied cases, the energy level of the triplet excited state of **NIN** could be about 1 eV below the singlet state,[24, 25] so that the energy of ^{3}**NIN** of approximately 2 eV is considerably higher than that of the triplet state of the porphyrin host (1.48 eV). The above data establish that energy-transfer processes from the excited states of **ZnH** to those of the same spin multiplicity of **NIN** are not allowed on a thermodynamic basis.

The bis(pyridyl)phenyldiimide guest **PIN** is almost insoluble in common organic solvents, but the energy levels of the excited states of **PIN** are expected to be higher than those of **NIN**, and hence the same arguments as above can be used to exclude the possibility of energy-transfer quenching from the porphyrin host to **PIN**.

Electrochemistry: The components of the complexes and the closely related free-base compounds were examined by cyclic voltammetry in DCM against a saturated calomel electrode (SCE). The results are collected in Table 1 and are typical for porphyrins and metalloporphyrins of this type.[26–27] Bisporphyrin **ZnH** has its first oxidation potential at +0.73 V, slightly higher than that of zinc tetraaryl porphyrins (+0.7 V under the same conditions). Fusion of the tetrazaanthracene moiety onto the zinc porphyrin macrocycle has little effect on the reduction potentials, but the derivative is slightly less easily oxidized than **Zn**.

Table 1. Cyclic voltammetry data[a] in CH_2Cl_2.

	Reduction [V]	Oxidation [V]
Zn	–, –1.40 (qr)	+0.7 (qr), +1.03 (qr)
FBB	–1.08 (r), –1.19 (r)	+0.98 (qr), –
ZnB	–1.11 (r), –1.40 (irr)	+0.72 (qr), +1.04 (ir)
FBH	–1.09 (r), –1.19 (r)	+0.98 (qr), –
ZnH	–1.14, –1.30 (r)	+0.73 (r), +0.97 (r)
ZnH-NIN	–0.44 (qr), –0.93 (qr)	
	–1.18 (r), –1.45 (ir)	+0.74 (qr), –

[a] r = reversible, qr = quasireversible, ir = irreversible.

The coupling of the porphyrin blocks to produce bisporphyrin cavities has no effect on the reduction and oxidation potentials in the free-base materials. However, in the zinc-containing compounds an increase in the first reduction potential is observed, but with a decrease in the second potential. A similar trend was also observed for the oxidation potentials of **ZnH** compared to **ZnB** (Table 1). Nonetheless, the lack of splitting observed for any of the potentials upon coupling indicates that the two porphyrinic units are electronically isolated from each other, in agreement with spectroscopic data.

The poor solubility of **NIN** and the insolubility of **PIN** in DCM prevented the preparation of solutions with convenient concentrations for electrochemical determinations. In these cases, the potentials of the diimide **NIN** were determined when complexed within **ZnH**, as discussed below. The redox potentials of **NIN** in DMF were reported to be –0.43 and –0.83 V versus SCE,[15] whereas for **PIN** previous determinations are lacking. For imides closely related to **NIN** a first reduction potential in polar solvents on the order of –0.55 V (vs SCE) is reported,[15, 23] and for compounds similar to **PIN** the reduction potential is more negative, about –0.8 V (vs SCE) in DCM.[9, 28]

Complexes

The bisporphyrin cavity **ZnH** has been successfully used for the complexation of suitably sized dipyridyl-functionalized guests.[29] The porphyrin center-to-center distance of 22 Å

0947-6539/02/0817-3940 $ 20.00+.50/0 *Chem. Eur. J.* **2002**, *8*, No. 17

within **ZnH** together with a zinc–pyridyl bond length of 2.2 Å, implies that optimally sized guests for complexation within **ZnH** have a distance of 17.6 Å or less between the complexation moieties. Modeling (AM1) of the diimide guests gave $N_{pyridyl}\cdots N_{pyridyl}$ distances of 15.9 Å (**NIN**) and 15.3 Å (**PIN**), and hence the cavity must collapse by less than 1 Å on each side for efficient simultaneous complexation to both metalloporphyrins.

Studies of complex formation by ^1H NMR spectroscopy: Complex formation between **ZnH** and **NIN** was initially examined by ^{1}H NMR spectroscopy, since this technique gives an indication of the geometry of the complex. Diimide **NIN** was only slightly soluble in DCM, yet was taken into solution on addition of one equivalent of **ZnH**, that is, complexation occurred indeed.

At 303 K the ^{1}H NMR spectrum of a solution containing a 1/1 mixture of **ZnH** and **NIN** showed signals for **NIN** protons that were significantly shifted upfield from those of uncomplexed **NIN**. In particular, the signals of the pyridyl ring protons were the most affected (α: $\delta = 2.98$, $\Delta\delta = -6.17$ ppm; β: $\delta = 5.58$, $\Delta\delta = -2.73$ ppm) owing to their close proximity to the magnetic anisotropy of the porphyrin ring. Such shifts have been used as diagnostic indicators for complex formation between metalloporphyrins and pyridyl nitrogen atoms.[29] The signals of the naphthalene ring protons of **NIN** were also shifted upfield ($\Delta\delta = -1.0$ ppm), but to a lesser extent than the pyridyl signals, consistent with their position within the complex. These results suggest the complexation geometry of **NIN** within **ZnH**, in which **NIN** is coordinated simultaneously to both metalloporphyrins.

The ^{1}H NMR signals of **NIN** at 303 K in the solution containing **ZnH**/**NIN** (1/1) were somewhat broader than those of **ZnH**. This broadening was removed when the solution was cooled to 263 K and below and indicates that some conformational change must be occurring within the complex in solution at ambient temperature. In contrast to the situation observed for **NIN** within the **ZnH-NIN** complex, the proton signals of **ZnH** are little affected by the addition of **NIN** to the solution (av $\Delta\delta = -0.06$ ppm).

In contrast to **NIN**, addition of the model diimide **NI** to a solution of **ZnH** in DCM did not result in any complexation-induced changes in the proton signals of either compound. This result was expected, since **NI** has no functional groups suitable for interaction with **ZnH**.

A similar situation to that observed for **NIN** was found for the phenyl diimide **PIN**. Addition of a solution of **ZnH** in chloroform to solid **PIN** caused the normally insoluble **PIN** to be taken into solution, that is, a complex was formed. At 303 K the ^{1}H NMR spectrum of a solution containing a 1/1 mixture of **ZnH** and **PIN** revealed signals for **PIN** shifted considerably upfield from their normal position. The most dramatically affected signals were again those of the pyridyl protons (α: $\Delta\delta = -6.06$ ppm; β: $\Delta\delta = -2.94$ ppm), in line with their proximity to the porphyrin walls of **ZnH**. The sinals for the phenyl protons of **PIN** was coincident with those of the aromatic protons of **ZnH** and could not be exactly identified. These results suggest a complexation geometry of **PIN** within **ZnH** with complexation to both metalloporphyrins of **ZnH**.

Examination of complex formation by optical spectroscopy: The formation of complexes between **ZnH** and the diimides was examined by UV/Vis and luminescence spectroscopy. Addition of increasing amounts of **NIN** to a solution containing a constant concentration of **ZnH** resulted in a shift to lower energy of the Soret and Q bands (Figures 1 and 2), typical of a zinc porphyrin axially coordinated to pyridyl residues.[30] The reference monoporphyrin **ZnB** displays, upon addition of similar amounts of **NIN**, absorption spectra which are the simple superposition of the individual components, without any spectral shift. Additivity in the absorption spectra is also observed when the model diimide **NI** is added to a solution of **ZnH** in toluene. In both cases these results indicate that no complexation occurs.

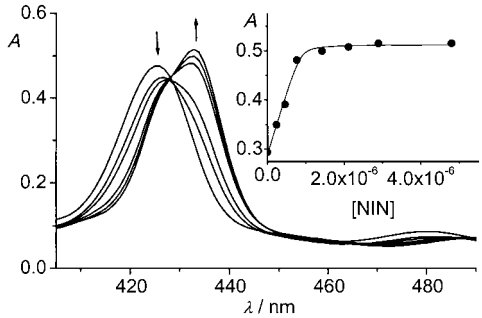

Figure 2. Effect of **NIN** addition on the absorption spectrum of **ZnH** in toluene (7×10^{-7} M). The concentrations of **NIN** were 0, 2.4×10^{-7}, 4.6×10^{-7}, 7.7×10^{-7}, 1.4×10^{-6} M, and 4.8×10^{-6} M. The inset shows the absorbance signal at 433 nm fitted to Equation (1), which yielded $K_{ass} = 7.2 \times 10^7\,M^{-1}$.

In Figure 2 the change in the absorption of the Soret band region of a **ZnH** solution with increasing addition of **NIN** is shown. The signal intensity at 433 nm is displayed in the inset of Figure 2 with fitting of the data according to Equation (1).[31]

$$Obs = Obs_0 + (\Delta Obs/2S_0)\{K_{dis} + X + S_0 - [(K_{dis} + X + S_0)^2 - 4XS_0]^{1/2}\} \quad (1)$$

Obs, which can be any observable, is absorbance in the present case; Obs_0 is the value of the observable at zero concentration of guest; S_0 is the constant concentration of the host **ZnH**; X is the variable concentration of guest; ΔObs is the maximum variation of the observable; and $K_{dis} = 1/K_{ass}$, where K_{dis} and K_{ass} are the dissociation and association constants, respectively. The association constant between **ZnH** and **NIN**, derived from the absorbance signal of **ZnH** (Figure 2) by using this procedure, is $K_{ass} = 7.2 \times 10^7\,M^{-1}$.

In the case of **PIN**, the insolubility of the guest in common solvents precluded a similar quantitative treatment. However, addition of solid **PIN** to a solution of **ZnH** in toluene gives rise (within 24 h) to a spectrum identical to that of **ZnH-NIN** (see Figure 1) and, therefore, may be assigned to the complex **ZnH-PIN**.

The emission spectrum of the porphyrin host is also affected by complexation of the diimide guests. In particular, the emission spectrum of **ZnH** in toluene displays a maximum at 660 nm, which is quenched by the addition of increasing amounts of **NIN** solution, as shown in Figure 3. When

  0947-6539/02/0817-3941 $ 20.00+.50/0

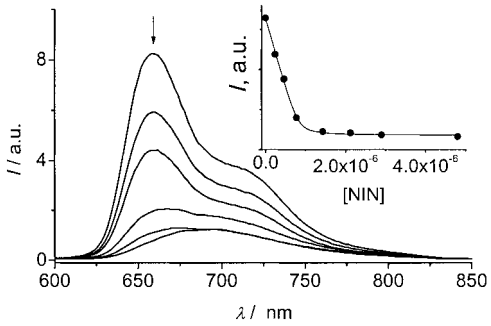

Figure 3. Effect of **NIN** addition on the emission spectrum of **ZnH** in toluene (7×10^{-7} M). The concentrations of **NIN** are the same as in Figure 2. In the inset the emission signal at 660 nm is fitted to Equation (1), which yielded $K_{ass} = 6.8 \times 10^{7}\,M^{-1}$.

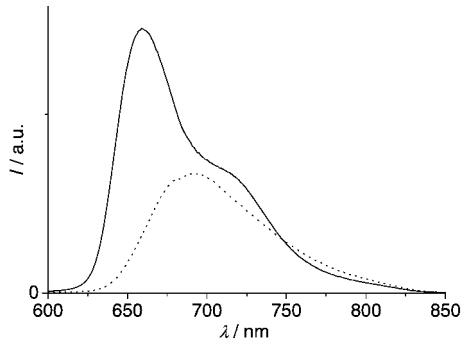

Figure 4. Emission spectrum of **ZnH** (——) and of **ZnH-MN** (••••) in toluene.

complexation is complete, the emission intensity of **ZnH** is strongly reduced, and the band at 690 nm may be taken as an indication of complex formation. The change in the emission intensity on addition of **NIN** can be treated according to Equation (1), and an association constant derived. The inset of Figure 3 plots the emission intensity at 660 nm against **NIN** concentration and yield. Treatment with Equation (1) gave an association constant of $6.8 \times 10^{7}\,M^{-1}$, in full agreement with the value obtained from the absorption data.

No effect on the luminescence of **ZnH** was detected on addition of model compound **NI** to the host solution; moreover, the reference monoporphyrin **ZnB** did not show any detectable change in emission spectrum on the addition of the same concentrations of **NIN**. This is again a clear indication that strong complexation occurs when two interaction sites are present.

With the phenyl diimide **PIN**, the complex **ZnH-PIN** was formed in 24 h on stirring a solution of **ZnH** (7×10^{-7} M) in toluene with solid **PIN** and yielded an emission spectrum that was identical (within experimental error) to that observed for the **ZnH-NIN** complex in solution.

The decrease in emission yield of **ZnH** observed in the complex on excitation of the porphyrin moiety can, in principle, be assigned either to quenching by the guest **NIN** or to a change in the photophysical properties of **ZnH** upon complexation. We recently reported that, in this type of azaanthracene-substituted porphyrin, axial complexation by pyridine causes a shift of the emission maximum to 690 nm and a reduction in the emission intensity to 0.034. The excited-state lifetime of **ZnH** is little affected by axial ligation by pyridine, and only a small decrease from 1.2 to 1.1 ns was observed.[20]

In a **ZnH** complex, the contributions to the overall luminescence decrease from intramolecular quenching processes or from coordination with pyridyl-type ligands can be evaluated by comparison with a bidentate pyridine reference guest with similar coordination properties to the present case, but with photo- and electrochemical properties unsuitable for quenching processes. The reference compound **MN** is complexed by **ZnH** to form **ZnH-MN** with an association constant of $7 \times 10^{7}\,M^{-1}$ according to absorption and emission spectroscopy.[32] Figure 4 shows the emission signals in toluene solution of **ZnH** (7×10^{-7} M) and of the complex **ZnH-MN**, formed in presence of **MN** (1×10^{-6} M). The maximum emission intensity of the complex was at 690 nm with an emission yield of 0.032, almost identical to that detected in the case of the complex formed between **ZnH** and monodentate pyridine ligands.[20] Complexation by the "innocent" (i.e., unable to quench the host emission by energy- or electron-transfer processes) guest **MN** by **ZnH** changes the luminescence properties of the host by decreasing the emission quantum yield and shifting the energy of the excited state to lower energy. Inspection of the data in Table 2, which lists the luminescence properties of the complexes **ZnH-MN**, **ZnH-NIN**, and **ZnH-PIN**, reveals that a further quenching mechanism is operative in the diimide complexes (see below).

Table 2. Luminescence properties of **ZnH** and complexes in toluene.

	298 K			77 K	
	λ_{max} [nm]	τ [ns]	ϕ[a]	λ_{max} [nm]	E [eV][b]
ZnH	660	1.2	0.043	666	1.86
ZnH-Pyr[c]	690	1.1	0.034	690	1.80
ZnH-NM	690	0.95	0.032	690	1.80
ZnH-NIN	690	0.080, 1[d]	0.008[f]	690	1.80
ZnH-PIN[e]	690	0.080, 1[d]	0.008[f]	690	1.80

[a] Emission quantum yield, see Experimental Section for details. [b] Energy from the emission maximum at 77 K. [c] Complex with pyridine, from ref. [20]. [d] The relative intensities are 95 and 5% for the fast and slow components, respectively.[33] [e] Only very dilute solutions could be measured with a bad signal-to-noise ratio.[34] [f] The luminescence yield is actually higher than expected on the basis of the reduction in lifetime (from 0.95 to 80 ps) because of the contribution to the luminescence of the longer-lived contaminants (see text).

Electrochemistry: The examination of the various complexes between **ZnH**, **NIN**, and **PIN** were hampered severely by the limited solubility of the diimides in DCM. In the case of **NIN**, sufficient solubility was obtained by complexation to allow measurements to be made, but for **PIN** this was not the case, and some assumptions were necessary (see below). The first redox potential measured in the complex **ZnH-NIN** (Table 1) is in agreement with that obtained for **NIN** in DMF with lithium perchlorate as electrolyte (– 0.43 V)[15] and is lower by at least 0.1 V than the value measured for similar naphthalenediimides without pyridyl substituents when free in solution.[15, 23] Complexation of **NIN** has a negligible effect on the oxidation potentials of **ZnH**, but increases both the first and second reduction potentials, owing to the electron-withdrawing nature of the bound imide.

  0947-6539/02/0817-3942 $ 20.00+.50/0 *Chem. Eur. J.* **2002**, *8*, No. 17

The reduction potentials of **PIN** could not be determined for solubility reasons. It is known that phenyl diimides are reduced at a potential more negative by approximately 0.25 V relative to the corresponding naphthalene derivatives.[7c, 11b] On the basis of the experimental value of 0.44 V for the first reduction of **NIN** in the complex **ZnH-NIN** (Table 1), a reduction potential of about 0.7 V (vs SCE) was assumed for the first reduction potential of **PIN** in **ZnH-PIN**.

Photoinduced processes in the complexes: Time-resolved emission and absorption spectroscopy is a powerful tool for identifying processes occurring in complexes of **ZnH** and the various guests. This technique allows the identification of the intermediates involved and the determination of the rates for the elementary processes in the complex.

The luminescence lifetime of **ZnH** in the model complex **ZnH-MN**, containing the innocent guest **MN**, was determined by excitation with the second harmonic ($\lambda = 532$ nm) of a Nd:YAG picosecond laser to be 0.95 ns.[32] The results of a similar experiment carried out with a solution of the complex **ZnH-NIN** in toluene are shown in Figure 5. The decay of the

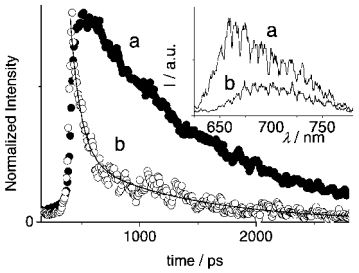

Figure 5. Normalized luminescence decay of **ZnH** in toluene following excitation with a 35 ps pulse (532 nm, 1 mJ) a) without and b) with **NIN**. The luminescence spectra in the time window 0 – 0.3 ns, displayed in the inset, are arbitrarily scaled.

luminescence intensity can be satisfactorily fitted by a double exponential with a major component (ca. 95 %) of 80 ps and a minor component (ca. 5 %) of about 1 ns.[33] The major luminescence component was assigned to quenching of **ZnH** luminescence by the guest **NIN**, while the minor component is consistent with a contribution from contamination by **ZnB** ($\tau = 1.2$ ns),[20] or by **ZnH** complexed by a nonquenching bispyridine-type contaminant ($\tau = 0.95$ ns).[32] The nature of the experiment is such as to give only an average of the lifetimes of the different contaminants, without the possibility of separating the various contributions. Attempts to further purify the host **ZnH** and the two guests **PIN** and **NIN** did not improve the above situation.

The fast and major component of the luminescence decay (80 ps) was assigned to a quenching process within the complex **ZnH-NIN** whose rate can be calculated from the equation $k = 1/\tau - 1/\tau_0$. In this case, τ_0 is the lifetime of the complex in the absence of a quenching process and was measured in the reference complex **ZnH-MN** to be 0.95 ns. Thus, the rate constant was calculated to be $k = 1.1 \times 10^{10}\ s^{-1}$. The emission spectrum of the complex **ZnH-NIN**, determined with a Streak Camera over the time window 0 – 300 ps, is shown in the inset of Figure 5 together with the spectrum of **ZnH** determined under the same conditions. While the spectrum of **ZnH** has a band at 660 nm, the complex exhibits a maximum at 690 nm, in full agreement with the spectra determined by steady-state methods (Figure 3) and with the spectrum of the complex **ZnH-MN** (Figure 4).

In conclusion, the complexation of **NIN** by **ZnH** results in the change of the photophysical properties of **ZnH**, in agreement with the effect of other pyridine-substituted guests and quenches the luminescence intensity within the complex. Similar time-resolved determinations were performed on solutions of the complex **ZnH-PIN**, and the results are in line with those observed for the **ZnH-NIN** complex. Also in this case, the intramolecular quenching of **ZnH** has a lifetime of 80 ps, which yields a quenching rate of $1.1 \times 10^{10}\ s^{-1}$, identical to that of **ZnH-NIN**. The luminescence properties are collected in Table 2.

Time-resolved absorbance experiments were also performed on solutions of the complexes **ZnH-NIN** and **ZnH-PIN** in an effort to gain information on the absorbing transient species. The absorption spectra detected at the end of a 35 ps laser pulse (532 nm) for solutions of **ZnH-NIN** and **ZnH** are shown in Figure 6. The band at 480 nm with a broad

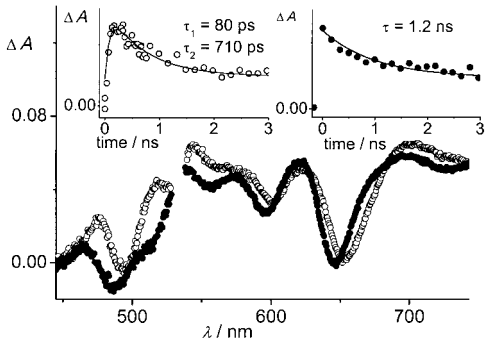

Figure 6. End-of-pulse spectra of **ZnH** in toluene without (●) and with **NIN** (○). Excitation with a 35 ps laser pulse, 532 nm, 4 mJ per pulse. In the insets the formation and decay at 515 nm of **ZnH**$^+$-**NIN**$^-$ (○) and the decay of ^{1}**ZnH** at 695 nm (●) are shown.

shoulder at 550 nm is similar to that of the 1,4,5,8-naphthalene diimide unit in the reduced form[23] and therefore this band was assigned to the anion **NIN**$^-$. The slight difference in the spectrum detected in this case (bands at 480 nm and in the region 510 – 560 nm) compared to that of 1,4,5,8-naphthalene diimide (bands at 480 and 610 nm with a shoulder at 510 nm),[23] can be accounted for by the effect of the pyridyl substituents. Figure 7 shows the end-of-pulse absorption spectra for solutions of **ZnH-PIN** and **ZnH**. The band around 720 nm is typical of the reduced form of phenyl imides closely related to **PIN**,[7b, 8, 9] and therefore this band was assigned to the anion **PIN**$^-$.

The insets in Figure 6 and 7 show the evolution with time of the absorption bands of the two anions at 515 and 728 nm, respectively. In the case of **ZnH-NIN**, the formation of the anion band with a lifetime of 80 ps and a decay with a lifetime of 710 ps were resolved. The former lifetime is identical to the decay of luminescence intensity and was assigned to forward electron transfer from the excited state of the complex

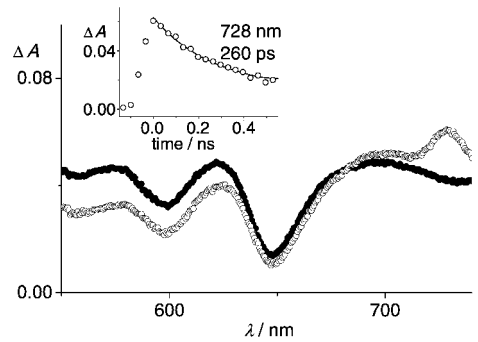

Figure 7. End-of-pulse spectra of **ZnH** in toluene without (●) and with **PIN** (○). A freshly prepared solution of **ZnH** (7×10^{-7} M) was stirred for 24 h over solid **PIN** before the experiment. Excitation with a 35 ps laser pulse, 532 nm, 4 mJ per pulse. In the inset the decay at 728 nm of **ZnH**$^+$-**PIN**$^-$ is shown.

localized on **ZnH** to the guest **NIN** to form a charge-separated state: ^{1}**ZnH-NIN** → **ZnH**$^+$-**NIN**$^-$. The lifetime of 710 ps was assigned to the decay of this charge-separated state, which recombines to the ground state (**ZnH**$^+$-**NIN**$^-$ → **ZnH-NIN**) as a result of electron back-transfer. The residual absorbance after the decay of the charge-separated state, which can be seen in the inset of Figure 6, was assigned to the triplet state of the complex, which can be monitored by using a different experimental setup with a longer timescale (see below).

For **ZnH-PIN**, the very dilute solutions employed[34] in conjunction with the signal-to-noise ratio typical of the experiment only allowed the decay of the anion band to be detected. A value for this decay of 260 ps was determined and assigned to the recombination of the charge-separated state **ZnH**$^+$-**PIN**$^-$. The residual absorbance of the solution after the decay of the anion was assigned to the triplet state of the complex.

Remarkably, in all of the complexes examined no absorbance features which could be assigned to the cation of the tetraazaanthracene-substituted porphyrin were observed; their time evolution should parallel that of the imide anions. Related aryl zinc porphyrin cations usually display bands around 650 nm, with an extinction coefficient of about 10^4 M^{-1} cm^{-1}.[35, 36] However, the singlet and triplet excited states of zinc porphyrins absorb in the same spectral region with similar absorption coefficients, and this often prevents the detection of a sizeable variation in the transient absorbance signal. This situation would appear to occur also for the zinc tetraazaanthracene-substituted porphyrin cation.

The triplet–triplet absorption spectrum of the complex **ZnH-NIN**, detected by a nanosecond flash photolysis system (490 nm excitation, 5 ns pulse duration, 2 mJ) displayed similar features to those of ^{3}**ZnH**,[20] which was characterized by broad absorption bands at 550 nm and 700 nm. However, the lifetime of the triplet excited state of the complex ^{3}**ZnH-NIN** in deaerated toluene solutions was 45 μs, considerably shorter than that of ^{3}**ZnH** (330 μs) under the same conditions. This fact must be ascribed to the perturbation of the triplet-state properties of the porphyrinic unit by complexation, similar to that shown to occur for the properties of the singlet excited state of the unit.[20] The yield of the triplet ^{3}**ZnH-NIN**, assuming similar molar absorption coefficients for ^{3}**ZnH** and ^{3}**ZnH-NIN**, was determined to be about 15% of that observed for the host **ZnH**. This reduction in yield is consistent with the presence of a process that depletes the population of the singlet excited state and is competitive with intersystem crossing, that is, the electron-transfer reaction occurring in the diimide complex. The triplet yield of the complex is in reasonable agreement with the 12% expected on the basis of the expression $\phi_c/\phi_0 = \tau_c/\tau_0$, in which ϕ_c and ϕ_0 are the triplet yields in the complex **ZnH-NIN** and in the host **ZnH**, respectively, and τ_c and τ_0 are the luminescence lifetimes in the complex **ZnH-NIN** and in the reference complex **ZnH-MN**, respectively. This result indicates that recombination of the charge-separated state does not yield a triplet state but produces ground-state products, in contrast with a previous observation reporting a partial recombination to a triplet state in a covalently linked system made of similar components.[7b]

Electron transfer: The levels of the excited states in Figure 8 were derived from the emission maxima of the complexes at 77 K, whereas the energy levels of the charge-separated states were derived from the electrochemical data in DCM, either

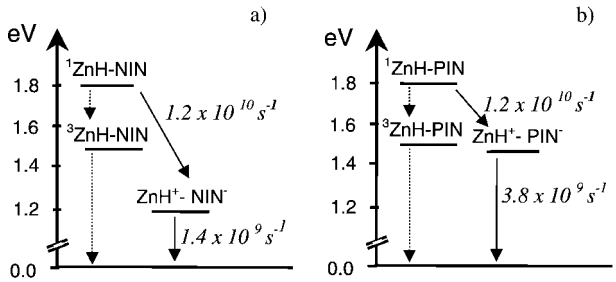

Figure 8. Schematic energy-level diagram and rates of the processes in the complexes a) **ZnH-NIN** and b) **ZnH-PIN**.

measured or assumed, without further corrections.[37, 38] This allows for the derivation of energies corresponding to 1.80 eV and 1.48 eV for the singlet and triplet excited states, respectively, and 1.18 eV and about 1.44 eV for for **ZnH**$^+$-**NIN**$^-$ and **ZnH**$^+$-**PIN**$^-$, respectively.

The classical treatment for nonadiabatic electron transfer[39] predicts a rate k_{el} described by Equation (2) where λ is the

$$k_{el} = \sqrt{(\pi/\hbar^2 \lambda k_B T)}\,|V|^2 \exp\left(\frac{-(\Delta G_0 + \lambda)^2}{4\lambda k_B T}\right) \qquad (2)$$

reorganization energy, k_B the Boltzmann constant, and ΔG^0 the standard free-energy change of the reaction. The pre-exponential includes the electronic matrix element V, which depends on the overlap of the electronic wave functions of the donor and acceptor groups, as well as the reorganization energy λ, whereas the exponential term is correlated to the standard free-energy change ΔG^0 and to the reorganization energy of the reaction λ. The latter can be expressed as the sum of two contribution: an inner and an outer part: $\lambda = \lambda_i + \lambda_o$. The parameter λ_i depends on internal differences in molecular structure (angles, distances, etc.) occurring within reaction partners as a consequence of the electron-transfer reaction, whereas λ_o is related to the ability of the solvent, through molecular orientation and polarization, to differently

  0947-6539/02/0817-3944 $ 20.00+.50/0 *Chem. Eur. J.* **2002**, *8*, No. 17

stabilize the initial and final states. It can be calculated according to Equation (3)[39] where e is the electron charge; ε_0

$$\lambda_o = e^2/4\pi\varepsilon_0(1/\varepsilon_{op} - 1/\varepsilon_s)(1/2r_A + 1/2r_D - 1/2r_{AD}) \quad (3)$$

is the permittivity of free space; ε_{op} and ε_s are the optical and static dielectric constants, respectively; and r_A, r_D, and r_{AD} are the radius of the donor, the radius of the acceptor, and the distance separating donor and acceptor, respectively.

Equation (2) predicts, for an homogeneous series of acceptors reacting with the same donor, the existence of a bell-shaped trend for the rate of energy transfer as a function of $-\Delta G^0$. The plot is characterized by a "normal" region for $-\Delta G^0 < \lambda$, in which the rate increases when the ΔG^0 of the reaction becomes more negative (i.e., the driving force increases); by an "activationless" region for $-\Delta G^0 = \lambda$, in which the maximum rate is achieved; and an "inverted" region for $-\Delta G^0 > \lambda$, in which the rate decreases with increasing $-\Delta G^0$. This classical approach has been refined by a semiclassical treatment that takes into account high-energy frequency vibrations and better describes the behavior in the "inverted" region.[40] The effect, in simple terms, is to decrease the steepness of the fall in the "inverted" part of the plot of k_{el} versus $-\Delta G^0$. Recently, the full bell-shaped trend was observed for electron transfer from the S_2 state of a porphyrin to an imide for a covalently linked dyad in a range of solvents.[41]

The electron-transfer reaction from the excited singlet state of the complexed tetraazaanthracene-substituted porphyrin chromophore to the imide, that is, the charge separation (CS), is characterized by $\Delta G^0 = -0.62$ eV and $\Delta G^0 \approx -0.36$ eV[42] for complexes **Zn-NIN** and **Zn-PIN**, respectively, and the measured rates are identical in the two cases ($1.1 \times 10^{10}\ s^{-1}$). Given the close similarities of the two imide acceptors used here, they can be considered as an homogeneous series displaying identical parameters in Equation (2), and from the insensitivity toward changes in the driving forces of the reactions in the two cases, it can be inferred that the reactions occur in the activationless region. From this behavior, an indicative λ value for the CS reaction on the order of 0.5 could be derived. The present results can be compared with the determination of the rates of CS reactions between a complete series of imides axially bound through a pyridyl substituent to a zinc porphyrin.[13] The imide series displayed variable redox potentials, the ΔG^0 for the electron-transfer process varied by 0.8 eV in CH_2Cl_2, and the rates in CH_2Cl_2 ranged from 6×10^7 to $5 \times 10^9\ s^{-1}$. The authors obtained satisfactory results by fitting the data according to Equation (2) with $\lambda = 0.8$ eV and $V = 0.3\ cm^{-1}$. This λ value, given the higher dielectric constant of CH_2Cl_2, is not in contradiction with the present suggested λ value for the CS reaction of about 0.5 eV in toluene. The absolute rate of $1.1 \times 10^{10}\ s^{-1}$ determined here lies in the range previously reported for similar systems involving an axial bond between an imide and a Zn porphyrin in DCM, for which values range from $5 \times 10^9\ s^{-1}$,[12, 13] to $2.1 \times 10^{10}\ s^{-1}$.[14] In contrast, the present rate is lower by a factor of about five than that determined in toluene for similar, but covalently linked systems separated by the same distance of 11 Å, as expected on the basis of the weaker coupling when a noncovalent bond connects the partners.[7b] The difference is larger (more than one order of magnitude in the same solvent) for a porphyrin-strapped imide, in which the electron acceptor, connected through flexible alkyl chains to both ends of the porphyrin, can likely approach close to the porphyrin donor.[43]

Charge recombination (CR) rates of 1.4×10^9 and $3.8 \times 10^9\ s^{-1}$ were determined from transient absorption experiments for **ZnH-NIN** and **ZnH-PIN**, respectively. The rate constants increase with increasing driving force: 1.18 eV for **ZnH**$^+$-**NIN**$^-$ → **ZnH-NIN** and about 1.44 eV for **ZnH**$^+$-**PIN**$^-$ → **ZnH-PIN**.[42] As discussed above, this is typical of normal-region behavior. A similar trend in CR rates was observed by Wasielewski et al. in dyads of a porphyrin analogue (zinc methyl 13^1-desoxopyropheophorbide) with naphthalenediimide and pyromellitimide, in which the distance separating the partners is identical to the present case (11 Å). In this case, the arrays displayed CR rates in toluene of $k_{CR} = 2.8 \times 10^9\ s^{-1}$ for the naphthalenediimide array with $\Delta G_o = -1$ eV, and $k_{CR} = 1.2 \times 10^{10}\ s^{-1}$ for the pyromellitimide dyad with $\Delta G_o = -1.27$ eV.[7b] Nearly identical results were reported by Osuka for dyads containing a Zn porphyrin linked through a boronate ester to the same diimides in benzene.[44] The absolute rates for charge recombination in covalently linked systems are faster, in analogy to that seen for the CS reactions above, due to the more efficient coupling provided by covalent bonds compared to the present case. Previously reported CR rates in nearly identical systems involving an axial coordinative bond between a Zn porphyrin and a pyridyl residue of a pyromellitimide in DCM are 9.4×10^8[12] and $1.3 \times 10^{10}\ s^{-1}$.[14] The reason for the difference in the above data is unclear. A comparison with the value of $k_{CR} = 3.8 \times 10^9\ s^{-1}$ for the phenylimide derivative **PIN** is difficult because of the different polarities of the solvents used and the differences in energetic and structural properties of the porphyrinic donor.

In spite of a rather high driving force for the recombination reaction, the behavior is typical of a normal region, in which the rate for CR increases with increasing driving force. This is indicative of a rather high λ associated with the CR reaction. The high λ value, in view of the low polarity of the solvent, is probably related to a rather important contribution from the internal reorganization energy λ_i. This large value for λ_i could likely be related to the distribution of charges in the cation of the unsymmetrical porphyrin chromophore, as compared to the ground state. A charge-transfer character has been actually evidenced for the lowest excited singlet state of the unit, and it could also be expected for the radical.[20] In this frame a large value of λ_i for the CR reaction would be in agreement with the suggested rather low λ value of 0.5 eV for the CS reaction, for which the distribution of charges in the initial (singlet excited state) and final (radical cation) state would be similar.

The results presented here show that the rate of electron transfer in these systems are decreased in comparison with similar covalently linked systems. The weaker interaction between components is effective both in the forward (CS) and in the back (CR) electron-transfer reaction. However, while the slowdown of the forward reaction leaves the efficiency of

  0947-6539/02/0817-3945 $ 20.00+.50/0

CS still around 90%, the lifetime of the charge-separated state is increased two- to threefold relative to covalently linked systems under similar conditions (solvent, donor–acceptor distance, thermodynamics),[7b, 44] and this makes the noncovalently linked system more appealing for the storage of light energy.

Conclusion

We have shown that a carefully designed bisporphyrin cavity can efficiently host properly functionalized diimide electron acceptors by metal–ligand interactions with a precise geometry. Photoinduced electron transfer between the host donor and the guest acceptor occurs efficiently, and the resulting charge-separated state displays a longer lifetime than similar covalently bound systems as a result of the weaker electronic coupling of the reaction partners.

Experimental Section

Host synthesis: Porphyrin block **FBB** (25 mg, 18 μmol) and 2-pyridyl *s*-tetrazine (3 mg, 13 μmol) were dissolved in the minimum amount of DCM along with triethylamine (5 drops), and the solution was pressurized at 14 kbar for 20 h. The solution was taken to dryness and pumped in vacuo to remove triethylamine and purified by chromatography (silica) with DCM/petroleum spirit (1/3) as eluent to give residual starting material, followed by $CHCl_3$/EtOAc (5%) to give **FBH** (10 mg, 52% based on porphyrin consumed). The product was recrystallized from DCM/MeOH. M.p. > 350 °C; MS: $m/z = 1465$ [M^{2+}+2H]; UV/Vis ($CHCl_3$): λ_{max} (ε) = 424 (783000), 462 (99000), 539 (31000), 610 (27000), 658 nm (4000); ^{1}H NMR (300 MHz, $CDCl_3$, 30 °C, TMS): $\delta = -2.43$ (br s, 4H; NH), 0.79 (d, ^2J(H,H) = 11 Hz, 2H; CH_2), 1.47 (s, 36H; *t*Bu), 1.51 (s, 36H; *t*Bu), 1.77 (d, ^2J(H,H) = 11 Hz, 2H; CH_2), 1.89 (s, 4H; CH), 1.97 (s, 4H; CH), 2.57 (s, 4H; CH), 4.04 (t, ^3J(H,H) = 3 Hz, 4H; CH), 6.32 (t, ^3J(H,H) = 3 Hz, 4H; CH), 7.45 (m, 2H; CH), 7.78 (t, ^4J(H,H) = 1.5 Hz, 4H; ArH), 7.96–7.91 (m, 12H), 8.00 (td, ^3J(H,H) = 7.5 Hz, ^4J(H,H) = 1.5 Hz, 2H; ArH), 8.06 (t, ^4J(H,H) = 1.5 Hz, 8H; ArH), 8.42 (s, 4H; ArH), 8.64 (d, ^3J(H,H) = 6 Hz, 2H; ArH), 8.73 (s, 4H; ArH), 8.86 (d, ^4J(H,H) = 3 Hz, 2H; ArH), 8.93 (d, ^3J(H,H) = 5 Hz 4H; ArH), 8.98 (d, ^3J(H,H) = 5 Hz, 4H; ArH).

ZnH synthesis: Bis-porphyrin host **FBH** was metalated with $CHCl_3$ and $Zn(Ac)_2$ (excess) in MeOH. The product was purified by column chromatography (silica) with $CHCl_3$ as eluent to give the bismetalated cavity **ZnH**, which was recrystallized from DCM/MeOH. M.p. > 350 °C; HR-ESMS calcd for $C_{202}H_{216}N_2Zn_2$ 1528.315 [M^{2+}+2H]; found: 1528.317; UV/Vis ($CHCl_3$): λ_{max} (ε) = 429 (697000), 487 (61000), 598 (18000), 646 nm (25000); ^{1}H NMR (300 MHz, $CDCl_3$, 30 °C, TMS): $\delta = 0.77$ (d, ^2J(H,H) = 11 Hz, 2H; CH_2), 1.43–1.52 (m, 144H; *t*Bu), 1.75 (d, ^2J(H,H) = 11 Hz, 2H; CH_2), 1.88 (s, 4H; CH), 1.96 (s, 4H; CH), 2.56 (s, 4H; CH), 4.04 (s, 4H; CH), 6.32 (t, ^3J(H,H) = 4Hz, 4H; CH), 7.45 (m, 2H; CH), 7.75 (t, ^4J(H,H) = 1.7 Hz, 4H; ArH), 7.90 (d, ^4J(H,H) = 1.7 Hz, 8H; ArH), 7.93 (t, ^3J(H,H) = 1.7 Hz, 4H; ArH), 7.99 (t of d, ^3J(H,H) = 7.4 Hz, ^3J(H,H) = 1.8 Hz, 2H; ArH), 8.03 (d, ^4J(H,H) = 1.7 Hz, 8H; ArH), 8.48 (s, 4H; ArH), 8.62 (m, 2H; ArH), 8.82 (s, 4H; ArH), 8.84 (m, 2H; ArH), 8.93 (s, 8H; ArH).

NMR spectroscopy: ^{1}H NMR spectra were recorded on Bruker spectrometers (300 or 400 MHz) at 303 K (unless otherwise stated) in $CDCl_3$ with standard Bruker pulse programs. Spectra were referenced to internal tetramethylsilane.

Electrochemistry: Cyclic voltammetry was carried out in DCM at ambient temperature with millimolar concentrations of compounds. The reference electrode was a saturated calomel electrode (SCE), and working and auxiliary electrodes were platinum. Tetrabutylammonium perchlorate (TBAP, 0.1M) was used as internal electrolyte, and the scan rate was 100 mV s^{-1}. Calibrated against ferrocene/ferrocenium (0.48 V).

Spectroscopic and photophysical studies: The solvents used were Spectroscopic Grade (C. Erba). Absorption spectra were recorded with a Perkin–Elmer Lambda 9 spectrophotometer, and emission spectra, uncorrected if not otherwise specified, were detected by a Spex Fluorolog II spectrofluorimeter equipped with a Hamamatsu R928 photomultiplier. Luminescence quantum yields ϕ for the samples, corrected for the photomultiplier response, were obtained with reference to the standard model **Zn** in toluene with $\phi = 0.08$.[36] Luminescence lifetimes in the range 20–2000 ps were determined by an apparatus based on an Nd:YAG laser (Continuum PY62–10) with 35 ps pulse duration, 532 nm, 1 mJ/pulse, and a Streak Camera.[45] Transient absorbance in the picosecond range made use of a pump-and-probe system based on an Nd:YAG laser (35 ps pulse, 532 nm, 2–4 mJ) and an OMA detector.[26] The instrumental response profile was obtained by measuring the buildup of the absorption of a solution of 3,3′-diethyloxadicarbocyanine iodide (DODCI) in methanol at 450 nm.[26] Zero time was assumed to be at the complete evolution of the absorption of the DODCI sample. T–T absorbtion spectra and lifetimes were determined by a laser flash photolysis apparatus based on a Nd:YAG laser (Surelite II, Continuum) coupled to an optical parametric oscillator (SL OPO Continuum) delivering 5 ns pulses of 2 mJ at 490 nm. Relative triplet yield in the complex was determined against **ZnH** under the same conditions, by assuming an identical molar absorption coefficient for the triplet state in the complex and the host. Experiments on triplet states were conducted in a home-made cuvette with 10 mm optical path, bubbled with argon for 5 min. Experiments at 77 K made use of quartz capillary tubes immersed in liquid nitrogen in a home-made quartz dewar. Estimated errors are 10% on lifetimes, 20% on quantum yields, and 30% on association constants.

Acknowledgements

This work was supported by CNR of Italy and by the Australian Research Council. The contribution of grant Agenzia2000 CNRC00B91D 004 to L.F. and of CQU Research Advancement Award Scheme (1999–2001) to M.R.J. are gratefully acknowledged.

[1] a) M. D. Ward, *Chem. Soc. Rev.* **1997**, *26*, 365–375, and references therein; b) T. Hayashi, H. Ogoshi, *Chem. Soc. Rev.* **1997**, *26*, 355–365, and references therein; c) C. J. Chang, J. D. K. Brown, M. C. Y. Chang, E. A. Baker, D. G. Nocera in *Electron Transfer in Chemistry*, *Vol. III*, part 2, (Ed.: V. Balzani), Wiley-VCH, Weinheim, **2001**, pp. 409–461; d) R. A. Haycock, A. Yartsev, U. Michelsen, V. Sundström, C. A. Hunter, *Angew. Chem.* **2000**, *112*, 3762–3765; *Angew. Chem. Int. Ed.* **2000**, *39*, 3616–3619.

[2] a) D. Gust, T. A. Moore, A. L. Moore in *Electron Transfer in Chemistry*, *Vol. III*, part 2, (Ed.: V. Balzani), Wiley-VCH, Weinheim **2001**, pp. 272–336, and references therein; b) H. Imamori, D. M. Guldi, K. Tamaki, Y. Yoshida, C. Luo, Y. Sakata, S. Fukuzumi, *J. Am. Chem. Soc.* **2001**, *123*, 6617–6628; c) A. Nakano, A. Osuka, T. Yamazaki, Y. Nishimura, S. Akimoto, I. Yamazaki, A. Itaya, M. Murakami, H. Miyasaka, *Chem. Eur. J.* **2001**, *7*, 3134–3151; d) K. Kilså, J. Kajanus, A. Macpherson, J. Mårtensson, B. Albinsson, *J. Am. Chem. Soc.* **2001**, *123*, 3069–3080; e) S. I. Yang, S. Prathapan, M. A. Miller, J. Seth, D. F. Bocian, J. S. Lindsey, D. Holten, *J. Phys. Chem. B* **2001**, *105*, 8249–8258; f) L. Flamigni, G. Marconi, I. M. Dixon, J.-P. Collin, J.-P. Sauvage, *J. Phys. Chem. B* **2002**, *106*, 6663–6671.

[3] a) C. A. Hunter, R. K. Hyde, *Angew. Chem.* **1996**, *108*, 2064–2067; *Angew. Chem. Int. Ed. Engl.* **1996**, 35, 1936–1939; b) F. Felluga, P. Tecilla, L. Hillier, C. A. Hunter, G. Licini, P. Scrimin, *Chem. Commun.* **2000**, 1087–1088; c) Y. Kuroda, K. Sugon, K. Sasaki, *J. Am. Chem. Soc.* **2000**, *122*, 7833–7834; d) T. B. Norsten, K. Chichak, N. Branda, *Chem. Commun.* **2001**, 1794–1795; e) H. Shinmori, T. Kajiwara, A. Osuka, *Tetrahedron Lett.* **2001**, *42*, 3617–3620.

[4] For example, see E. Kaganer, E. Joselevich, I. Willner, Z. Chen, M. J. Gunter, T. P. Jeynes, M. R. Johnston, *J. Phys. Chem. B* **1998**, *102*, 1159–1165.

[5] For example, see a) A. M. Brouver, C. Frochot, F. G. Gatti, D. A. Leigh, L. Mottier, F. Paolucci, S. Roffia, G. W. H. Wurpel, *Science*, **2001**, 219, 2124–2128; b) P. R. Ashton, R. Ballardini, V. Balzani, A. Credi, K. R. Dress, E. Ishow, C. J. Kleverlaan, O. Kocian, J. A. Preece,

N. Spencer, J. F. Stoddart, M. Venturi, S. Wenger. *Chem. Eur. J.* **2000**, *6*, 3558 – 3574.
[6] L. Flamigni, M. R. Johnston, *New J. Chem.* **2001**, 1368 – 1370.
[7] a) M. P. O'Neil, M. P. Niemczyk, W. A. Svec, D. Gosztola, G. L. Gaines III, M. R. Wasielewski, *Science* **1992**, *257*, 63 – 65; b) G. P. Wiederrecht, M. P. Niemczyk, W. A. Svec, M. R. Wasielewski, *J. Am. Chem. Soc.* **1996**, *118*, 81 – 88; c) H. Levanon, T. Galili, A. Regev, G. P. Wiederrecht, W. A. Svec, M. R. Wasielewski, *J. Am. Chem. Soc.* **1998**, *120*, 6366 – 6373; d) R. T. Hayes, M. R. Wasielewski, D. Gosztola, *J. Am. Chem. Soc.* **2000**, *122*, 5563 – 5567.
[8] a) A. Osuka, S. Nakajima, K. Maruyama, N. Mataga, T. Asahi, I. Yamazaki, Y. Nishimura, T. Ohno, K. Nozaki, *J. Am. Chem. Soc.* **1993**, 115, 4577 – 4589; b) A. Osuka, H. Yamada, K. Maruyama, N. Mataga, T. Asahi, M. Ohkouci, T. Osaka, I. Yamazaki, Y. Nishimura, *J. Am. Chem. Soc.* **1993**, 115, 9439 – 9452.
[9] H. Himamori, K. Yamada, M. Hasegawa, S. Taniguchi, T. Okada, Y. Sakata, *Angew. Chem.* **1997**, *109*, 2740 – 2742; *Angew. Chem. Int. Ed. Engl.* **1997**, *36*, 2626 – 2629.
[10] Q. Tan, D. Kuciauskas, S. Lin, S. Stone, A. More, T. A. More, D. Gust, *J. Phys. Chem. B*, **1997**, *101*, 5214 – 5223.
[11] a) H. Shiratori, T. Ohno, K. Nozaki, A. Osuka, *Chem. Commun.* **1999**, 2181 – 2182; b) H. Shiratori, T. Ohno, K. Nozaki, I. Yamazaki, Y. Nishimura, A. Osuka, *J. Org. Chem.* **2000**, *65*, 8747 – 8757; c) T. Yamazaki, I. Yamazaki, A. Osuka, *J. Phys. Chem. B*, **1998**, *102*, 7858 – 7865;
[12] C. A. Hunter, J. K. M. Sanders, G. S. Beddard, S. Evans, *J. Chem. Soc. Chem. Commun.* **1989**, 1765 – 1766.
[13] J. Otsuki, K. Harada, K. Toyama, Y. Hirose, K. Araki, M. Seno, K. Takatera, T. Watanabe, *Chem. Commun.* **1998**, 1515 – 1516.
[14] K. Yamada, H. Imamori, E. Yoshizawa, D. Gosztola, M. R. Wasielewski, Y. Sakata, *Chem. Lett.* **1999**, 235 – 236.
[15] C. J. Zhong, W. S. Kwan, L. L. Miller, *Chem. Mater.* **1992**, *4*, 1423 – 1428.
[16] R. A. Dine-Hart, W. W. Wright, *Makromol. Chem.* **1971**, *143*, 189 – 206.
[17] R. N. Warrener, D. Margetic, R. A. Russell, *Synlett.* **1998**, 585 – 587.
[18] R. N. Warrener, D. Margetic, unpublished results.
[19] R. N. Warrener, M. R. Johnston, M. J. Gunter, *Synlett.* **1998**, 593 – 595.
[20] L. Flamigni, G. Marconi, M. R. Johnston, *Phys. Chem. Chem. Phys.* **2001**, *3*, 4488 – 4494.
[21] The energy of the excited states is derived from the maximum of emission at 77 *K*.
[22] T. C. Barros, S. Brochsztain, V. G. Toscano, P. B. Filho, M. J. Politi, *J. Photochem. Photobiol. A* **1997**, *111*, 97 – 104.
[23] S. R. Greenfield, W. A. Svec, D. Gosztola, M. R. Wasielewski, *J. Am. Chem. Soc.* **1996**, *118*, 6767 – 6777.
[24] S. Green, M. A. Fox, *J. Phys. Chem.* **1995**, *99*, 14752 – 14757.
[25] V. Wintgens, P. Valat, J. Cossanyi, *J. Chem. Soc. Faraday. Trans.* **1994**, *90*, 411 – 421.
[26] L. Flamigni, N. Armaroli, F. Barigelletti, V. Balzani, J.-P. Collin, J.-O. Dalbavie, V. Heitz, J.-P. Sauvage, *J. Phys. Chem.* **1997**, *101*, 5936 – 5943.
[27] R. Beavington, P. L. Burn, *J. Chem. Soc. Perkin Trans. 1.* **2000**, 1231 – 1240.
[28] In ref. [9] the potentials are reported relative to ferrocene/ferrocenium (Fc/Fc^+); they have been scaled relative to SCE by using a Fc/Fc^+ potential of 0.47 V vs SCE in DCM.
[29] M. R. Johnston, M. J. Gunter, R. N. Warrener, *Chem. Commun.* **1998**, 2739 – 2740.
[30] For example, see: a) E. B. Fleischer, A. M. Shachter, *Inorg. Chem.* **1991**, *30*, 3763 – 3769; b) C. C. Mack, N. Bampos, J. M. K. Sanders, *Angew. Chem.* **1998**, *110*, 3169 – 3172; *Angew. Chem. Int. Ed.* **1998**, *37*, 3020 – 3023; c) N. Armaroli, F. Diederich, L. Echegoyen, T. Abisher, L. Flamigni, G. Marconi, J.-F. Nierengarten, *New J. Chem.* **1999**, *23*, 77 – 83; d) J. Brettar, J.-P. Gisselbrecht, M. Gross, N. Solladie, *Chem. Commun.* **2001**, 733 – 734.
[31] a) C. S. Wilcox, in *Frontiers in Supramolecular Organic Chemistry and Photochemistry* (Eds.: H.-J. Schneider, H. Dürr), VCH, Weinheim, **1991**, p. 123; b) S. Encinas, K. L. Bushell, S. M. Couchman, J. C. Jeffery, M. D. Ward, L. Flamigni, F. Barigelletti, *J. Chem. Soc. Dalton Trans.* **2000**, 1783.
[32] L. Flamigni, A. M. Talarico, F. Barigelletti, M. R. Johnston, *Photochem. Photobiol. Sci.* **2002**, *1*, 190 – 197.
[33] In the fitting of the luminescence decay, zero time was taken as the full evolution of the emission. The full width at half maximum (FWHM) of the laser pulse is 35 ps, but the full duration of the pulse is about 65 ps, at which time the short component of 80 ps has partially decayed within the pulse. The pre-exponentials of 95 % for the major component and of 5 % for the minor component were estimated from an extrapolation of the decays back to the middle time of the laser pulse.
[34] The preparation of more concentrated samples by contact of solid **PIN** with **ZnH** solutions requires several days at ambient temperature, and this results in partial degradation of the components.
[35] J. Fajer, D. C. Borg, A. Forman, D. Dolphin, R. H. Felton, *J. Am. Chem. Soc.* **1970**, *92*, 3451 – 3459.
[36] I. M. Dixon, J.-P. Collin, J-P. Sauvage, L. Flamigni, *Inorg. Chem.* **2001**, *40*, 5507 – 5517.
[37] Taking into consideration the corrections for Coulombic stabilization and change in solvent dielectric constant according to Weller,[38] a correction of + 0.012 eV should be applied to the CS energy level, well below the approximation involved in the present case.
[38] A. Weller, *Z. Phys. Chem.* **1982**, *133*, 93 – 98.
[39] R. A Marcus, N. Sutin, *Biochim. Biophys. Acta* **1985**, *811*, 265 – 322 and references therein.
[40] J. Jortner, *J. Chem. Phys.* **1976**, *64*, 4860 – 4867.
[41] N. Mataga, H. Chosrowjan, Y. Shibata, N. Yoshida, A. Osuka, T. Kikuzawa, T. Okada, *J. Am. Chem. Soc.* **2001**, *123*, 12 422 – 12 423.
[42] ΔG^0 is derived from an assumed value of − 0.7 eV for the reduction potential of **ZnH-PIN**.
[43] R. J. Harrison, B. Pearce, G. S. Beddard, J. A. Cowan, J. K. M. Sanders, *Chem. Phys.* **1987**, *115*, 429 – 448.
[44] H. Shiratori, T. Ohno, K. Nozaki, I. Yamazaki, Y. Nishimura, A. Osuka. *Chem. Commun.* **1998**, 1539 – 1540.
[45] L. Flamigni, *J. Phys. Chem.* **1993**, *97*, 9566 – 9572.

Received: February 5, 2002 [F3851]